Pattern Roughness Mitigation of 22 nm Lines and Spaces: The Impact of a H_2 Plasma Treatment

Peter De Schepper,* Alessandro Vaglio Pret, Ziad el Otell, Terje Hansen, Efrain Altamirano-Sanchez, Stefan De Gendt

As the semiconductor industry pursues Moore's law, the demand to obtain smaller features continues. Extreme ultraviolet (EUV) lithography remains one of the primary options for sub-20 nm patterns. However, the technology struggles to meet the line width roughness (LWR) specifications. In this article, we present the significance of plasma treatment as a roughness smoothing technique. Two EUV photoresists with 22 nm lines are exposed to various plasma processes. We highlight the advantages of a hydrogen plasma treatment and its vacuum ultraviolet (VUV) emission as an optimal smoothing process and discuss the effect of photoresist thickness, initial LWR and the VUV plasma emission. Even though a H_2 plasma treatment results in a successful reduction of LWR/LER, the target value of below 2nm is not yet achieved.

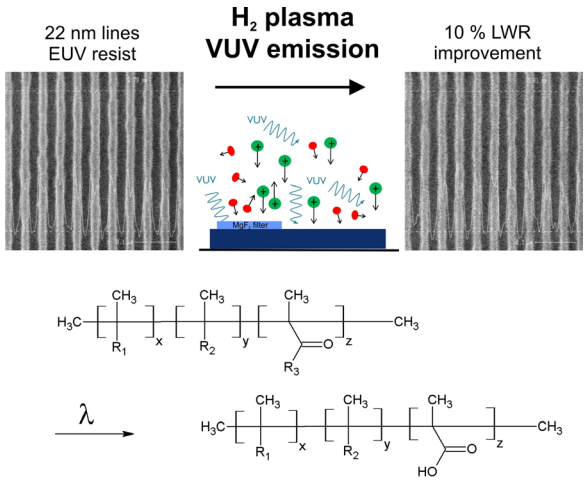

1. Introduction

Extreme UV-lithography (EUV) needs to be competitive for the definition of features with sub-20 nm dimensions. Therefore, source, mask, infrastructure, and photoresist materials continuously need to improve to keep pace with the resolution, LWR and sensitivity performance required by the IC technology. Polymer properties and composition; such as polymeric side groups, photo-acid generator (PAG) loading, quencher loading, as well as photoresist thickness are key factors to improve this resolution performance.

Even though significant improvements have been made, LWR continues to be a major challenge. Post-lithographic techniques, such as plasma treatment, have experimentally demonstrated the improvement of feature roughness. Plasma smoothing has caught interest since the introduction of 193 nm related polymers.[1] The use of these treatments allows us to modify both the bulk and surface properties of specific polymer layers. These modifications, mainly side group depletion, and polymer cross linking and chain scission, have an impact on both surface and sidewall roughness.[2]

The synergy of both vacuum ultraviolet (VUV) radiation and reactive species has already been proven to induce chemical modifications to polymer films, which in turn influences the critical dimensions (CD) and edge variability along the defined lines.[3,4] The impact of VUV irradiation has been studied extensively before.[5,6] Besides the important effect of VUV-emission, the interaction of reactive ions with the substrate plays a significant role.

P. De Schepper, Dr. Z. el Otell, Dr. T. Hansen, Prof. S. De Gendt
Department of Chemistry, Katholieke Universiteit Leuven (KULeuven), Kapeldreef, 3001 Leuven, Belgium
P. De Schepper, Dr. Z. el Otell, Dr. E. Altamirano-Sanchez, Prof. S. De Gendt
Department of Unit Process and Modules, IMEC, Kapeldreef 75, 3001 Leuven, Belgium
E-mail: peter.deschepper@imec.be
Dr. A. Vaglio Pret
KLA-Tencor Corp., ICOS/PSG, Research Park Haasrode 1112, Esperantolaan 8, 3001 Leuven, Belgium

Plasma Process. Polym. **2014,** DOI: 10.1002/ppap.201400078

The interactions between ions and organic layers have been already reported, highlighting the importance of the ion energy and flux.[2,3,7–9] If the ion energy is high enough, ions induce surface modifications and create a densified or even carbonized top layers. Végh et al.[10] simulated the formation of a 1–2 nm damage layer, heavily cross-linked by dehydrogenation, by using 100 eV Ar-ions on a polystyrene substrate.

Nevertheless, plasma treatment in general is making slow progress and no sub-2 nm results have been reported for 193 nm photoresist materials so far. Thus, a drastic improvement on line edge roughness (LER) and LWR for EUV resist materials is needed to meet the International Technology Roadmap for Semiconductors (ITRS) specifications.[11] Therefore, exposing EUV-resists to various plasma processes with and without optical blocking windows allows to assess separately the influence of both ultraviolet irradiation and reactive species.

This paper highlights the impact of photoresist chemistry, various plasma treatment approaches on 22 nm lines and in doing so, confirms the importance of hydrogen plasma treatment in Section 3.1 and 3.2. Furthermore, Section 3.3 and 3.4 point out the plasma smoothing limitations for resist-patterning using EUV lithography.

2. Experimental Section

2.1. Plasma Sources

The experiments were performed in two types of 300 mm etch reactors from LAM Research. The majority of the experiments were performed in an ICP reactor while a limited number of experiments were carried out in a CCP reactor. The first etch tool is the Kiyo 3× and is an inductively coupled plasma (ICP) source. This high density plasma reactor uses a planar coil on top of a quartz window and is powered through a matching network at 13.56 MHz. The bottom electrode was, depending on the experiment, either biased or kept at ground potential to gain control of the ion energy independently from the ion density. The walls (60 °C), top window (120 °C), and electrostatic chuck (ESC) (20 °C) were kept at a constant temperature.

The second etch tool is a dual-frequency capacitive coupled plasma (2f-CCP) source, the Lam Exelan reactor. The lower electrode is powered by two independent power supplies with 2 and 27 MHz frequencies. The top-electrode (Si) was grounded and kept at a temperature of 80 °C during the experiments. The inter-electrode gap is 2.3 cm and the wafer area pressure was tuned by means of adjusting the vertical position of a series of confinement rings. The ESC was kept at a constant temperature of 60 °C.

In both reactors, the pressure, gas flow, bias power, and chemistry (H_2, HBr, Ar, He, and mixtures) were changed to evaluate the impact on line width roughness.

2.2. Vacuum Ultraviolet Spectrometer Configuration

Spectra in the EUV and VUV wavelength range were obtained using a VUV spectrometer (model 234/302, McPherson made). The spectrometer is equipped with two gratings, 1 200 and 2 400 gratings. The so-called 1 200 grating has a wavelength range from 30 to 550 nm with a resolution of 0.1 nm at a wavelength of 313.1 nm. The wavelength range and resolution for the 2 400 grating are 30–275 and 0.06 nm, respectively. These gratings can be exchanged without breaking the vacuum. The adjustable slits at both the plasma and detector side were set to 0.85 mm. The spectrometer itself was pumped down by an EXT turbomolecular pump (Edwards vacuum) to a pressure below 10^{-4} mbar.

Emission was detected by means of a sodium salicylate coated window and a photomultiplier tube (PMT). The detector housing (model 658, McPherson made) contains the sodium salicylate coated window to convert VUV light into the visible wavelength range suitable for the PMT (R6095, produced by Hamamatsu). The PMT voltage was set to 1 200 V. The PMT current was measured with a picoammeter (model 6485, Keithley). Typically, 2 500 data points were obtained with an integration time of 60 ms per point.

To assess the effect of VUV photons only on LWR, a magnesium fluoride (MgF_2) optical filter was placed onto the resist surface before loading into the plasma reactor.[12] The MgF_2 window has an optical cut-off wavelength of 120 nm allowing only transmittance and interaction of VUV photons above 120 nm.

The VUV emission from a hydrogen plasma, generated in the LAM Kiyo 3× reactor, at a pressure of 15 mTorr with 1 800 W input power and 100 sccm gas flow, was recorded with and without the MgF_2 window. A comparison of these measured spectra was performed in order to confirm the cut-off wavelength of this filter between 100 and 400 nm.

2.3. Extreme Ultraviolet Photoresist Samples and Lithographic Exposure

To obtain 30 and 22 nm lines and spaces, two state-of-the-art 40 and 50 nm thick EUV resists were exposed on the ASML NXE:3100 EUV tool installed at Imec. Numerical aperture of 0.25 with conventional and dipole illumination were used to define the 30 and 22 nm lines, respectively. These organic materials have already been defined and characterized previously and are labeled as EUV-A and EUV-B.[12] The 13.5 nm features were obtained using ArF lithography in combination with Direct-Self Assembly, as reported in reference.[13]

2.4. Metrology

On-line capturing of images was performed by Hitachi CG4000 scanning electron microscope (SEM) to estimate the CD and LWR of photoresist patterns before and after plasma treatment. Briefly, a large set of top-view images is captured using a beam current of 8 pA and accelerating voltage of 300 V. The parameters were chosen to reduce the resist damaging while preserving the S/N ratio and respecting the ITRS requirements. A rectangular scanning mode is used to acquire SEM images with a 512×512 pixel resolution. This mode allows to obtain different magnifications in x and y direction, 300 000 and 49 000, respectively. The field of view is $0.450 \times 2.755\ \mu m^2$ giving a pixel size of $0.88 \times 5.38\ nm^2$. In total, 32 frames are captured. The SEM images are then analyzed off-

DOI: 10.1002/ppap.201400078

line using the Terminal PC software from Hitachi and LERDEMO software, developed by Demokritos National Center for Scientific Research.[14,15] The LERDEMO software calculates the correlation length (ξ), Hurst exponent (α), as well as the power spectral density (PSD) using the height–height correlation function (HHCF). It is possible to demonstrate that the area subtended by the PSD is proportional to σ_{LER}^2 by using the Parseval theorem.[16] In this way, it is possible to assess the roughness evolution before and after the plasma treatment by comparing the area below the curve.

For this study, per measured die, typically 30–50 images with 4–5 lines each are averaged to reduce the intrinsic noise characteristic of the PSD and roughness analysis. This noise is more visible in the low frequency (LF) region because of the longer line length and thus less sampling points.

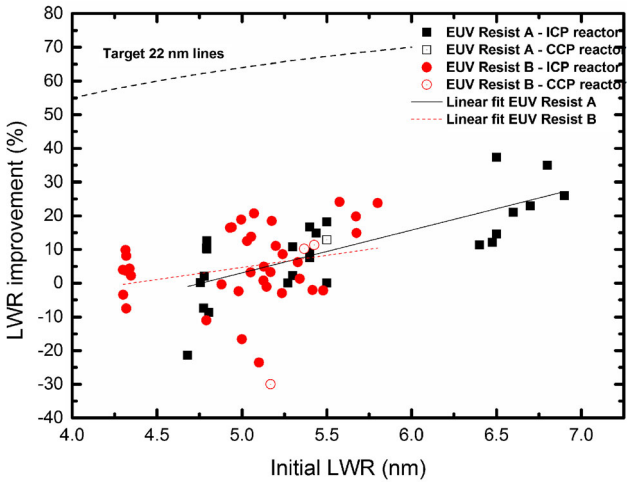

Figure 1. LWR improvement of 22 nm half pitch lines as a function of the initial roughness for the two different photoresists. Photoresist A (closed squares) is a PMMA related platform and photoresist B (open circles) is a PS/PMMA co-polymers. For both datasets a linear fit was achieved. The full line represents the fit for EUV Photoresist A while the dotted line highlights the linear trend of Photoresist B. In addition the target for 22 nm lines is presented.

3. Results and Discussion

It is important to emphasize the effect of plasma smoothing on 22 nm lines. Therefore, over 100 experiments with various initial LWR are evaluated in order to highlight the impact of new and published plasma processes on state-of-the art patterns.[8,17,18] The complete dataset is based on results obtained by exposing 22 nm lines to various process conditions. These variable conditions are enumerated in the experimental section and will be briefly explained subsequently. The use of a diverse set of plasma chemistries is based upon the availability of reactive species and photons within the plasma. For instance, HBr, Ar, He, and H_2 provide us with a large window of photon energies capable of modifying organic materials.[12] On the other hand, heavy Ar and Br ions will react differently with the organic surface compared to smaller H-ions and radicals.[1,19] Moreover, to expand the dataset, two types of EUV photoresist are included as well. These resists are used to assess the impact of the lithographic polymer chemistry on the smoothing capability of the plasma technique.[12] Based on the experimental dataset, it was only possible to draw conclusions on results obtained in the ICP reactor. The limited number of experiments performed in the CCP reactor does not allow any comparison of the effect of different reactors on the resist improvement.

3.1. Plasma Smoothing of 22 nm Lines

Figure 1 shows a comparison of the LWR improvement as a function of the initial LWR of the two EUV resists, A and B. The figure shows the role of the initial roughness and its effect on the plasma smoothing technique. The positive values indicate an improvement of the LWR while the negative values suggest an aggravation of it. Both resists show a decreasing roughness improvement with decreasing initial LWR, obtaining at best a 10% improvement for an initial LWR of 4.3 nm. The linear fit of both datasets shows this decreasing trend. By comparing the slopes of these fits, it can be noticed that photoresist A is apparently more rapidly losing its smoothing capabilities compared to resist B. This could probably be related to the different chemical composition of the resists. Photoresist A is related to an acrylic resist platform while resist B is similar to a polystyrene/polymethylmethacrylate (PS/PMMA) copolymer.[12] Ester functionalities are known to detach fast because of the plasma's VUV emission. Therefore, resist A is "degrading" faster than polymer B while photoresist B has a slightly larger process window for LWR improvement.

Besides the LWR improvement, it is important to maintain the profile of the resist line after the plasma treatment, which allows further pattern transfer into the underlying substrates. Figure 2 shows the evolution of the post-treatment LWR as a function of the post-treatment CD. Starting with 22 nm lines, the goal of plasma treatment is reducing the roughness but maintaining the CD within a 1 nm 3σ process window represented by the two vertical dotted lines. Within this process window a minimum LWR of 4.2 nm is reached. Nevertheless, a further reduction of the LWR towards 3.8 nm is possible for EUV resist B. But, this roughness improvement comes with a reflow of the resists profile resulting in a 20% increase in the CD. A trade-off in the LWR improvement and pattern profile is thus required. Both resists show a reflow trend after plasma treatment, which could be linked to the LWR improvement.

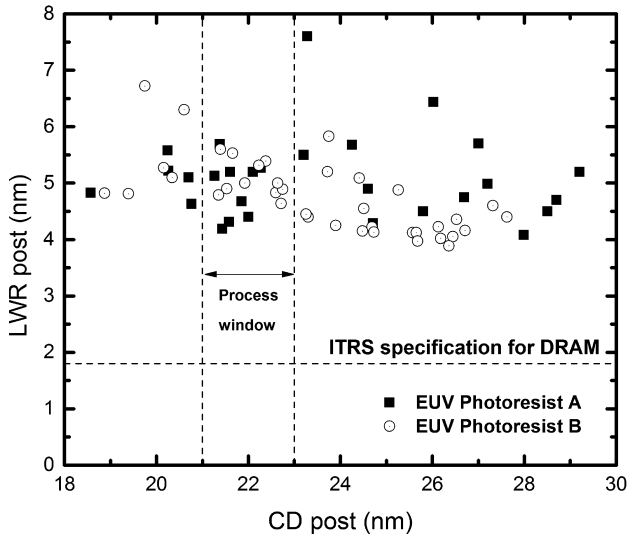

Figure 2. LWR mitigation of 22 nm lines after plasma treatment as function of CD after treatment for the two different resists. The horizontal dashed line is the required ITRS specifications for DRAM. The two vertical dotted lines represent the CD process window.

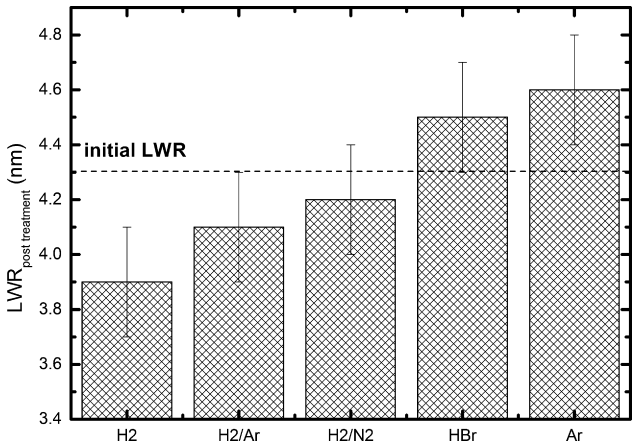

Figure 3. LWR improvement of photoresist B for different plasma processes highlighting the importance of H_2 plasma treatment. The initial LWR is plotted as a dotted line and the improvement for various plasma processes is represented by the bars.

For both Figure 1 and 2, it can be concluded that the PMMA and PS/PMMA copolymer substrates react comparably to these plasma treatments.

3.2. The Effect of H_2 Plasma Treatment

The superiority of a H_2 plasma treatment compared to the other processes was already highlighted in literature.[12] But, it is good to confirm and reproduce these statements. Therefore the 22 nm lines are exposed to various plasma processes. For all these processes a 300 W TCP power, 100 sccm total gas flow, and a reactor pressure of 10 mTorr are used. Photoresist B was treated for 30 s while resist A only for 10 s, as this exposure time gives the best LWR improvement.[10]

Figure 3 shows a comparison on the improvement of the LWR. Only the results of photoresist B are plotted in this figure, as the trend for the photoresist A is identical. These results are in agreement with previous reported results and it can be concluded that for 22 nm lines and spaces printed in EUV resist, hydrogen plasma treatment has the highest improving effect.

However, it is necessary to understand if process optimization of the hydrogen treatment will yield further improvement. Accordingly, Figure 4 and 5 show the same dataset as presented in Figure 1 emphasizing now on the plasma chemistry. In order to maintain a good overview, the results for both resists are separated. The datasets were plotted in order to compare non-hydrogen (Ar, HBr,...) processes versus hydrogen treatments. The hydrogen process window is influenced by changing pressure, power, and process time. Nevertheless, both figures do not show a further process improvement compared to the results highlighted in Figure 3. In addition, these hydrogen plasma data points follow a similar trend as the one highlighted in Section 3.1 where the induced smoothing is limited by its initial LWR.

As already highlighted in Figure 2, it is important to preserve the line profile after plasma treatment while optimizing the LWR. Figure 6 shows the LWR improvement as function of the change in CD focusing on the effect of hydrogen plasma treatment where the dotted lines indicate

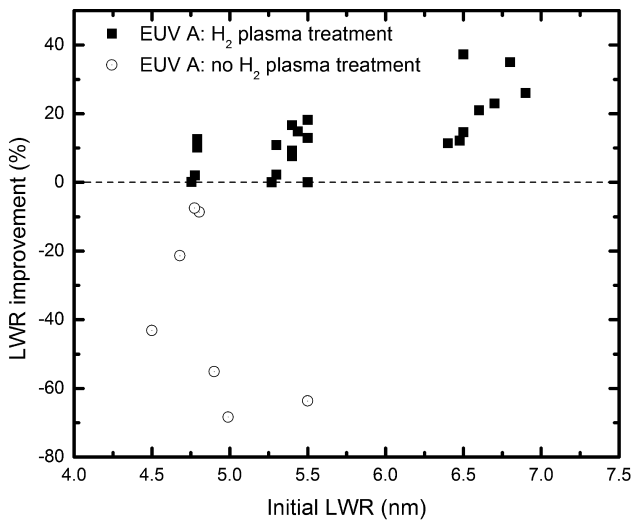

Figure 4. LWR improvement as a function of the initial LWR for EUV photoresist A. The results obtained using a H_2 plasma (black squares) and other chemistries such as He, HBr, Ar, and N_2 (open circles) are compared.

DOI: 10.1002/ppap.201400078

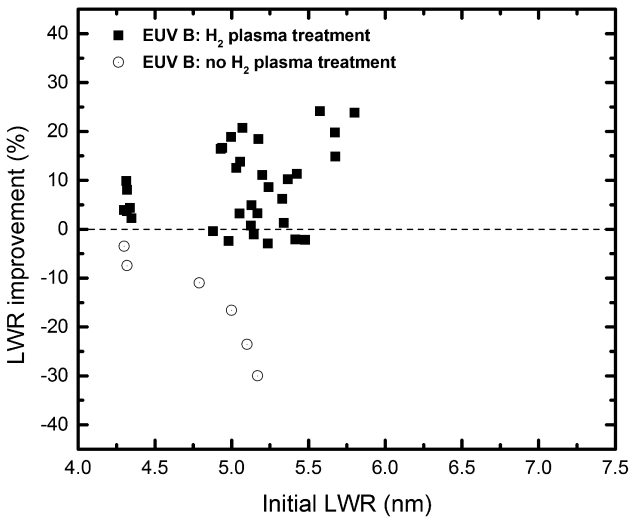

Figure 5. LWR improvement as a function of the initial LWR for EUV photoresist B. The results obtained using a H_2 plasma (black squares) and results using another plasma chemistry such as He, HBr, Ar, and N2 (open circles) are compared.

the initial conditions. An ideal working plasma process should be capable of reducing the LWR and preserving the CD of the lines. This change of the CD after the plasma treatment is shown in Figure 6. The results obtained with a hydrogen plasma are compared to those obtained using other chemistries for both resist platforms. Although hydrogen causes the largest LWR improvement, this treatment induces also resist reflow. The reflow provokes profile loss and an increase of the CD.[12]

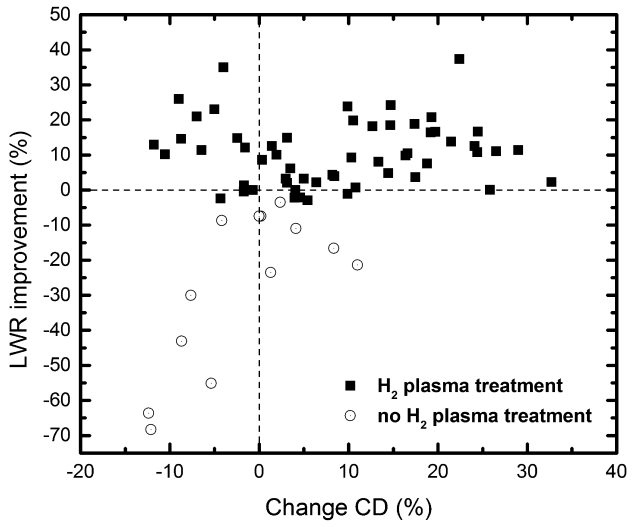

Figure 6. CD and LWR changes for 22 nm lines after plasma treatment. The data emphasizes the difference between plasma processes using hydrogen (black) or other chemistries (open circles).

Three conclusions can be drawn based on the experimental results presented in Section 3.1 and 3.2. Firstly, a better LWR improvement process is obtained with a hydrogen plasma compared to other plasma chemistries. Secondly, LWR improvement seems to converge to a minimum value of only 3.8 nm for 22 nm lines after plasma treatment (Figure 2). Finally, Figure 1, 4, and 5 show a trend whereby the LWR improvement reduces with decreasing initial LWR, independently of the considered photoresist.

3.3. The Effect of H_2 Plasma VUV-Emission on CD Changes

It is clearly stated that a H_2 plasma treatment achieves the best results in the presented experimental dataset. Both the reactive plasma species as well as the VUV photons within different wavelength ranges are interacting with the organic material. Therefore, it is important to understand separately the effect of VUV photon emission and reactive species produced by H_2 plasmas. In order to differentiate their effects, an MgF_2 optical window is used to expose the resist only to photons and shield it from the reactive plasma species.

Figure 7 shows the change of CD as a function of LWR improvement where the dotted cross lines show the initial status before plasma treatment. The influence of the VUV emission by the plasma is emphasized by plotting the results of full exposed versus shielded 22 nm lines. Since H_2 plasmas have typically strong VUV-emission between 120 and 150 nm due to their atomic and molecular transitions,[20] the introduction of an MgF_2 window is suitable to study the effect of plasma VUV emission only above 120 nm. VUV-emission below 120 nm

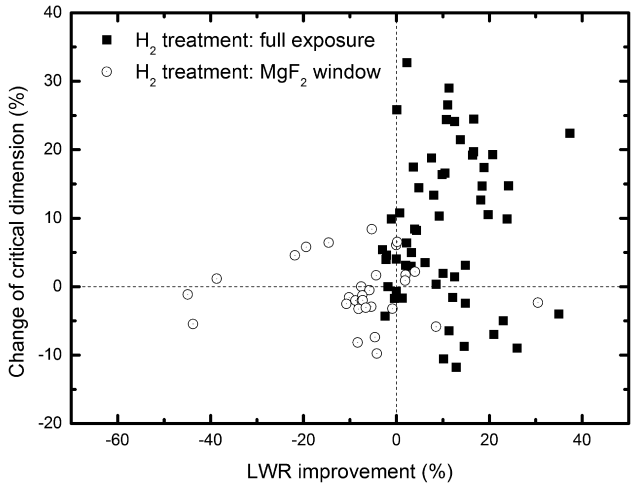

Figure 7. CD and LWR changes with and without the MgF_2 optical filter. The best results can be found in the bottom-right part of the graph.

and reactive species would have been included in the full plasma–polymer interaction if not for this window.

The data in Figure 7 is in line with the previous results and highlights the lack of LWR improvement when the resist is shielded from plasma species and only exposed to the VUV-emission.[12,21] Based on this outcome, it was initially assumed that VUV-emission above 120 nm does not play a significant role in LWR improvement. However, this is in contradiction with results obtained in the literature.[17,22–25] Therefore, using the VUV spectrometer, the plasma emission between 100 and 300 nm was measered with and without the MgF_2 window.

Figure 8 compares these two measured spectra. It can be seen that roughly 10–30% of the plasma VUV emission intensity between 120 and 160 nm is transmitted. This large loss in plasma emission can possibly explain the limited capability of LWR improvement. It is most likely that higher photon intensity could play a significant role in the modifications of the photoresists.

To understand the influence of all VUV photons as they are interacting during normal plasma conditions, 28 nm lines printed in EUV resist B were shielded with the MgF_2 optical window and exposed to the best working hydrogen plasma process as defined in Section 3.2. The measurements, presented in Figure 8, show that on average 20% of all photons are transmitted through this window in the wavelength range of interest (100–160 nm). Therefore, the process time was extended five times to a plasma process of 150 s for this experiment. In this way, the total photon intensity can be mimicked to that during a full plasma exposure without the optical window. The results of this experiment are analyzed with the help of PSD and plotted in Figure 9. The black curve represents the 30 s full plasma

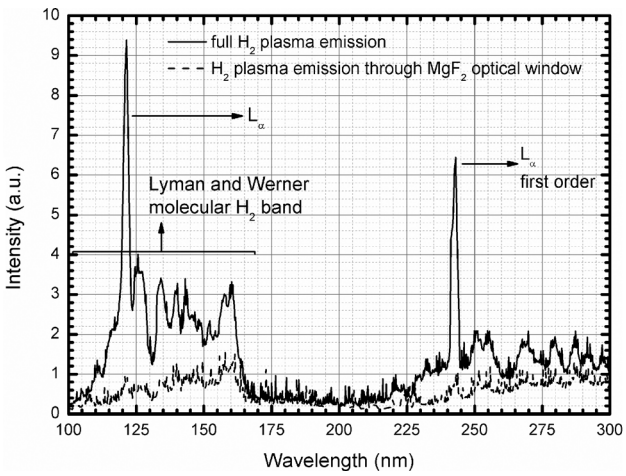

Figure 8. VUV emission between 100 and 300 nm without (solid line) and with (dashed line) a MgF2 optical window. For this experiment a plasma with input power of 1 200 W and 100 sccm of H_2 at a pressure of 15 mTorr was used.

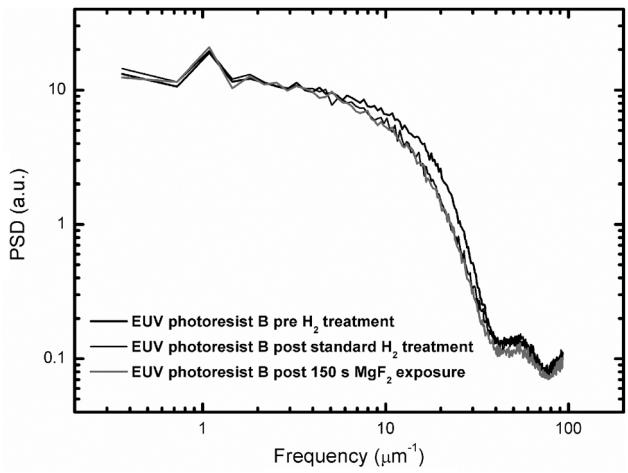

Figure 9. PSD analysis of 28 nm lines printed in EUV photoresist B before (bold black) and after the H_2 plasma treatment. The lines exposed only to the VUV photons result in the grey PSD plot compared to the full plasma exposure plotted in black.

exposure while the gray graph highlights the results for the MgF_2 shielded lines. It can be concluded that both processes result in almost identical LWR improvement. Thus, the VUV photons generated during the hydrogen plasma are the main components influencing the roughness mitigation. As shown in Figure 9, this roughness improvement is obtained in the mid and high frequency region, confirming previous observations.[25–27] The low frequency roughness on the other hand is only marginally changed exposing the resist to the full plasma treatement. Next to the LWR improvement, it is important to mention that the resist lines undergo a slight reflow of 6% for the samples exposed to the full plasma, while no reflow is observed for the VUV-only treated samples. These results emphasize also the importance of other reactive species and their influence on the reflow mechanism.

3.4. Plasma Smoothing Limitations

As previously reported and confirmed by our experimental dataset, H_2 plasma treatment has the largest positive impact in terms of LWR improvement.[12] However, the smoothing effect of 30% with respect to the initial condition reached for 30 nm half pitch does not seem to be achievable for 22 nm, where only 10% improvement is obtained. This raises an important question on which factors are causing this dramatic lack of performance at smaller feature size. An experimental study was performed to answer this question, and the results are reported in the following section.

Not only pattern dimensions decrease with the evolution of lithographic technology, also LWR improves with this evolution. The effect of the hydrogen plasma treatment

with decreasing initial LWR is touched upon in Section 3.1 and 3.2. It is reasonable to say that the effect of H_2 plasma treatment is dependent on the initial LWR. This dependency is shown in Figure 10 whereby LWR improvement becomes less significant for features with a lower initial LWR. The EUV-A photoresist material is used to print the 22 nm lines while almost identical resist is used for the 30 nm lines. Both PMMA materials slightly differ in the composition of the PAG and not in polymer backbone. It is well documented that the VUV photons emitted by the plasma have a drastic impact on the ester and lactone groups present in acrylate photoresist back bones causing chain scissioning. This allows a reorganization of the polymer chain that favors roughness.[28] Thus, the effect of the plasma treatment onto both platforms should be comparable. On the other hand, the DSA developed 13.5 nm lines are poly styrene (PS) based and therefore reacts differently to the applied plasma treatment. However, the focus of Figure 10 and 11 is at the effect of plasma curing and its impact for various technology nodes. These figures compare state of the art EUV processes and resists, who evolve over time, comparing actual, and up to date process conditions. As a consequence, the best process conditions

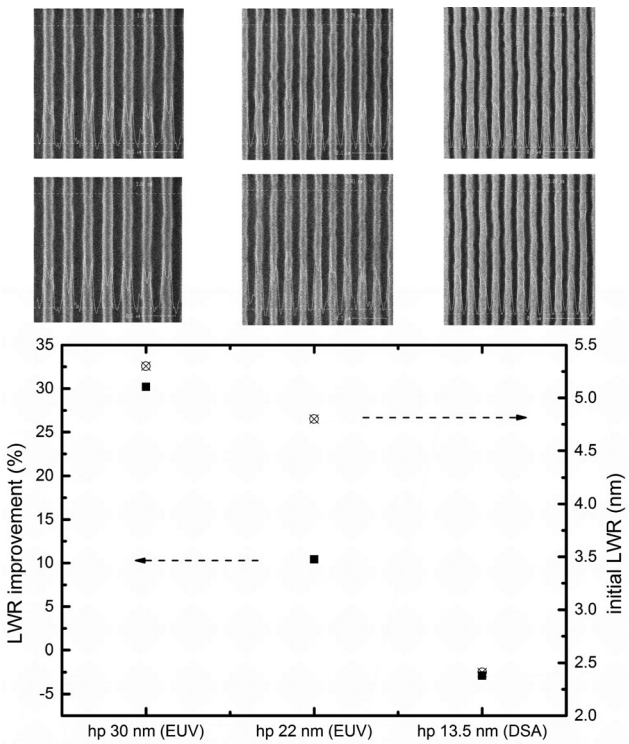

Figure 10. TOP [images]: is a set of top- down CD-SEM images captured with Hitachi H4000. On the left 30 nm, center 22 nm, and right 13.5 nm lines after exposure (top) and after plasma smoothing (bottom). BOTTOM [graph]: shows the correlation between LWR improvement (full squares) and the initial LWR (open circles) in function of the feature size.

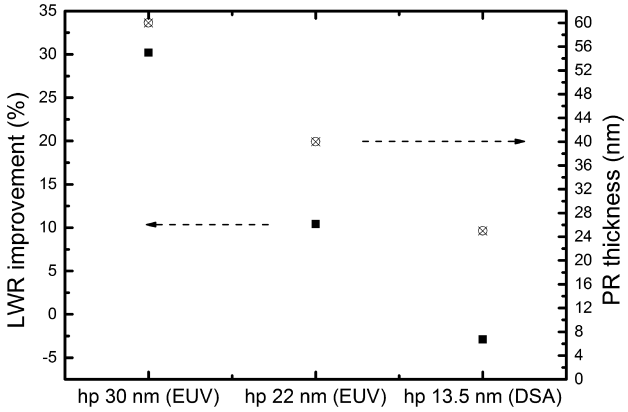

Figure 11. This graphs shows the correlation between LWR improvement (full squares) and photoresist thickness (open circles) in function of the feature size.

are used to develop both 30 and 22 nm lines and were used to compare their capability of LWR reduction after plasma treatment. This difference in process conditions also implies that the LWR after lithography differs depending on the technology node.

On the other hand, to maintain high performance for very small patterns, the thickness of these materials scales down as well with the features to avoid failure mechanisms, such as pattern collapse. Figure 11 highlights the correlation between initial LWR and photo resist thickness showing a similar trend.

4. Discussion

Although the LWR variations are within the CD-SEM accuracy (0.2 nm 3σ for LWR and 0.6 nm 3σ for CD values), all measurements were repeated at least twice and the same LWR and CD changes were observed.[14]

Firstly, the improvement capabilities are slightly different for the two chemically different EUV photoresists. Both resists show 193 nm resist technology characteristics, such as ester functionalities and specific high carbon containing or cyclic functional side groups. These photocleavable groups are sensitive to the VUV emission from the plasma. The experiments suggest that the presence of such groups within these EUV polymers makes it possible to modify the polymer's bulk and surface properties to improve the LWR.

Furthermore, hydrogen plasma treatment is highlighted as best working process within the presented dataset to reduce the LWR. VUV only has shown to be responsible for the complete LWR improvement, but it seems that the exposure to other plasma species triggers a reflow process. The VUV photons are able to penetrate in the full resist layer and are able to cleave most of the

photosensitive groups.[3] We tend to believe that it is the lack of photonflux in other experimental plasma processes, which limits their impact on LWR. Next to the bulk changes induced by the VUV photons, ions and radicals are able to react with the surface and subsurface.

It may be suggested that next to this synergetic reaction there are other contributing factors. The substrate temperature, glass transition temperature T_g, radius of gyration R_G and polymer end-to-end distance R_{EE} could play a significant role as well.[25,29]

Finally, we believe that the "available" amount of photoresist material and more specific the amount of ester functionalities limits the roughness reduction. Scaling down from 30 nm lines to 22 nm lines means that the total photoresist volume is reduced by almost 40%. On contrary to acrylate based materials, PS is not very sensitive to VUV exposure.[1] Therefore, the reduction of the amount of ester functionalities (in terms of volume for 30 and 22 nm lines) towards zero (for the DSA material) can be directly correlated to the limiting LWR mitigation. Moreover, the combination of a larger resist volume and lower initial roughness, is a requirement to tackle further roughness reduction by plasma enhanced and sustained polymer modifications. For the completion of this study, the comparison of identical resists with equeal initial LWR but various resist thicknesses will be added in future work.

Ultimately, initial LWR is an important factor (shown in Figure 4, 5, and 10) for LWR improvement and a succesfull etch pattern transfer. Further improvement of sub-2 nm LWR is very challenging with current resist materials. A critical aspect is the resist LWR (at least for the chemically amplified photoresists), which is governed by the low frequencies.

5. Conclusion

By evaluating over 100 plasma experiments on 22 nm lines exposed on two types of EUV resist, it has been confirmed that hydrogen plasma treatments have superior smoothing capability. It was seen that the best achievable LWR after plasma treatment is only 3.8 nm, which is still far above the ITRS specifications.

To emphasize the influence of VUV emission above 120 nm, a MgF_2 optical filter was used. Initial results obtained with this optical filter indicate a lower change of the LWR. However, it was difficult to fully comprehend the impact of VUV emission on roughness improvement, as a part of the VUV was absorbed by the window. The processing time was increased by fivefolds to make up for this absorption. The results then showed that VUV emission only is capable of improving the LWR just as much as the full plasma exposure induces.

Finally, we highlight the LWR improvement and its dependency on the initial roughness. Also, LWR improvement is correlated to the initial amount of photoresist material and ester functionalities. Further refining on the process and more controlled parameters are being optimized to enhance this process. In combination with the use of model resists and an in depth characterization of photoresist modification, a complete LWR mechanism will be presented.

Acknowledgements: The authors would like to thank Philippe Foubert, BT Chan, Vladimir Samara, and Jean-Francois de Marneffe for useful discussions.

Received: May 8, 2014; Revised: July 17, 2014; Accepted: August 6, 2014;DOI: 10.1002/ppap.201400078

Keywords: 22 nm line; H_2 plasma treatment; LWR limitations; VUV plasma emission

[1] G. S. Oehrlein, R. J. Phaneuf, D. B. Graves, *J. Vac. Sci. Technol. B: Microelectron. Nanom. Struct.* **2011**, *29*, 1.
[2] F. Weilnboeck, R. L. Bruce, S. Engelmann, G. S. Oehrlein, D. Nest, T.-Y. Chung, D. Graves, M. Li, D. Wang, C. Andes, E. A. Hudson, *J. Vac. Sci. Technol. B: Microelectron. Nanom. Struct.* **2010**, *28*, 5.
[3] D. Nest, T.-Y. Chung, D. B. Graves, S. Engelmann, R. L. Bruce, F. Weilnboeck, G. S. Oehrlein, D. Wang, C. Andes, E. A. Hudson, *Plasma Process. Polym.* **2009**, *6*, 10.
[4] T.-Y. Chung, D. B. Graves, F. Weilnboeck, R. L. Bruce, G. S. Oehrlein, M. Li, E. A. Hudson, *Plasma Process. Polym.* **2011**, *8*, 11.
[5] A. Hollander, R. Wilken, J. Behnisch, *Surf. Coatings Technol.* **1999**, 116.
[6] A. Hollander, J. Behnisch, *Surf. Coatings Technol.* **1998**, *98*, 855.
[7] S. Engelmann, R. L. Bruce, M. Sumiya, T. Kwon, R. Phaneuf, G. S. Oehrlein, C. Andes, D. Graves, D. Nest, E. A. Hudson, *J. Vac. Sci. Technol. B: Microelectron. Nanom. Struct.* **2009**, *27*, 1.
[8] S. Engelmann, R. L. Bruce, T. Kwon, R. Phaneuf, G. S. Oehrlein, Y. C. Bae, C. Andes, D. Graves, D. Nest, E. A. Hudson, P. Lazzeri, E. Iacob, M. Anderle, *J. Vac. Sci. Technol. B: Microelectron. Nanom. Struct.* **2007**, *25*, 4.
[9] L. Ling, X. Hua, X. Li, G. S. Oehrlein, E. A. Hudson, P. Lazzeri, M. Anderle, *J. Vac. Sci. Technol. B: Microelectron. Nanom. Struct.* **2004**, *22*, 6.
[10] J. J. Végh, D. Nest, D. B. Graves, R. Bruce, S. Engelmann, T. Kwon, R. J. Phaneuf, G. S. Oehrlein, B. K. Long, C. G. Willson, *J. Appl. Phys.* **2008**, *104*, 3.
[11] International Technology Roadmap for Semiconductors, www.itrs.net, **2013**.
[12] P. De Schepper, T. Hansen, E. Altamirano-Sanchez, A. Vaglio Pret, W. Boullart, S. De Gendt, *Proc. SPIE* **2013**, *8685*, 868508.
[13] P. A. Rincon Delgadillo, R. Gronheid, C. J. Thode, H. Wu, Y. Cao, M. Somervell, K. Nafus, P. F. Nealey, *Proc. SPIE* **2012**, *8323*, 83230D.
[14] A. V. Pret, R. Gronheid, T. Ishimoto, K. Sekiguchi, *J. Micro/Nanolith. MEMS MOEMS* **2010**, *9*, 4.

[15] G. P. Patsis, V. Constantoudis, N. Tsikrikas, E. Gogolides, *J. Microlith. Microfab. Microsys.* **2004**, *3*, 429.
[16] Y. Wei, R. L. Brainard, *Advanced processes for 193 nm immersion lithography*, SPIE, Bellingham, WA, USA **2009**.
[17] E. Pargon, M. Martin, K. Menguelti, L. Azarnouche, J. Foucher, O. Joubert, *Appl. Phys. Lett.* **2009**, *94*, 10.
[18] M. Brihoum, R. Ramos, G. Cunge, K. Menguelti, E. Pargon, O. Joubert, *J. Appl. Phys.* **2013**, *113*, 1.
[19] E. Pargon, K. Menguelti, M. Martin, a. Bazin, O. Chaix-Pluchery, C. Sourd, S. Derrough, T. Lill, O. Joubert, *J. Appl. Phys.* **2009**, *105*, 9.
[20] H. Abgrall, E. Roueff, F. Launay, J.-Y. Roncin, J.-L. Subtil, *J. Mol. Spectrosc.* **1993**, *157*, 512.
[21] E. Altamirano-Sánchez, A. Vaglio Pret, R. Gronheid, W. Boullart, *Proc. SPIE* **2012**, *8328*, 83280L.
[22] Y. Inatomi, T. Kawasaki, M. Iwashita, *Proc. SPIE* **2006**, *6153*, 61533X.
[23] K. Takeda, H. Asahara, T. Hanawa, K. Tsujita, H. Okumura, *J. Photopolym. Sci. Technol.* **2003**, *16*, 4.
[24] M. Yamaguchi, T. Wallow, Y. Yamada, R.-H. Kim, J. Kye, *J. Photopolym. Sci. Technol.* **2008**, *21*, 5.
[25] E. Pargon, L. Azarnouche, M. Fouchier, K. Menguelti, J. Jussot, *J. Vac. Sci. Technol. B: Microelectron. Nanom. Struct.* **2013**, *31*, 6.
[26] P. De Schepper, A. Vaglio Pret, E. Altamirano-Sánchez, Z. el Otell, S. De Gendt, *Proc. SPIE* **2014**, *9054*, 90540C.
[27] L. Azarnouche, E. Pargon, K. Menguelti, M. Fouchier, D. Fuard, P. Gouraud, C. Verove, O. Joubert, *J. Appl. Phys.* **2012**, *111*, 8.
[28] E. Pargon, L. Azarnouche, M. Fouchier, K. Menguelti, R. Tiron, C. Sourd, O. Joubert, *Plasma Process. Polym.* **2011**, *8*, 12.
[29] G. P. Patsis, V. Constantoudis, E. Gogolides, *Microelectron. Eng.* **2004**, *75*, 3.